≥2.8 log units above the Ni-NiO buffer. Although the fO_2 in subduction zones is likely to be higher than 1 log unit below the Ni-NiO buffer [B. J. Wood, L. T. Bryndzia, K. E. Johnson, *Science* **248**, 337 (1990)], our measured fO_2 is probably unrealistically high. However, because our modal assemblages and mineral compositions are similar to those obtained in experiments on a synthetic olivine basalt, buffered to Ni-NiO (*19*), we suggest that the difference in fO_2 has little effect on phase relations.

14. D. Walker, M. A. Carpenter, C. M. Hitch, *Am. Mineral.* **75**, 102 (1990); D. Walker, *ibid.* **76**, 1092 (1991).
15. The 75-kbar starting compositions were designed with a high structural water content so that capsules would be easier to seal. The basaltic composition was a mixture of 50% MORB glass and 50% blueschist. The blueschist is sample 719805 from the Department of Mineral Sciences, Smithsonian Institution [S. S. Sorenson, *Geol. Soc. Am. Mem.* **164**, 59 (1986)]. The basanitic composition was a mixture of 50% blueschist and 50% kaersutite. The kaersutite is from Soda Springs, Arizona [C. Cross and J. R. Holloway, *Geol. Soc. Am. Abstr. Prog.* **6**, 437 (1964)].
16. F. C. Hawthorne, in *Amphiboles and Other Hydrous Pyriboles - Mineralogy*, vol. 9A of *Reviews in Mineralogy*, D. R. Veblen, Ed. (Mineralogical Society of America, 1981), pp. 103–139; B. Velde, *Am. Mineral.* **63**, 343 (1978); K. Langer and M. Raith, *ibid.* **59**, 1249 (1974); A. Le Cleac'h and P. Gillet, *Eur. J. Mineral.* **2**, 43 (1990); C. Chopin *et al.*, *ibid.* **4**, 67 (1992).
17. Chemical formulae were calculated by summing cations exclusive of Ca, Na, and K to 13, or all cations except K to 15, if the former method yielded an M4 cation deficiency.
18. P. M. Black, *Tectonophysics* **43**, 89 (1977). The typical high-pressure, low-temperature amphibole found in many relict subduction zones is glaucophane, but its upper thermal stability is ≤550°C between 10 and 25 kbar [W. V. Maresch, *ibid.* **43**, 109 (1977)], and therefore it should not be stable at the conditions of our experiments. Amphiboles produced in other studies of the melting of basalt and peridotite are typically hornblende, that is they have a significant A-site occupancy. This contrasts to the low A-site occupancy of our amphiboles; however, the other amphiboles were produced at higher temperatures than ours.
19. S. Poli, *Am. J. Sci.*, in press.
20. C. Chopin, *Bull. Mineral.* **106**, 715 (1983); G. A. Chinner and J. E. Dixon, *J. Petrol.* **14**, 185 (1973).
21. In two experiments at 25 kbar for a starting material of the lawsonite-bearing blueschist seeded with eclogite, lawsonite broke down at 675°C but not at 650°C.
22. R. C. Newton and G. C. Kennedy, *J. Geophys. Res.* **68**, 2967 (1963).
23. K. D. Watson and D. M. Morton, *Am. Mineral.* **54**, 267 (1969).
24. S. M. Peacock, *Geol. Soc. Am. Bull.*, in press.
25. K. Yamamoto and S. Akimoto, *Am. J. Sci.* **277**, 288 (1977).
26. This work was supported by National Science Foundation grants EAR 8904261, EAR 9205061, EAR 8408163 (electron microprobe facility) and EAR 8915759 (FTIR facility).

7 December 1992; accepted 4 March 1993

Pliocene Paleoclimate and East Antarctic Ice-Sheet History from Surficial Ash Deposits

David R. Marchant, Carl C. Swisher III, Daniel R. Lux, David P. West, Jr., George H. Denton

The preservation, age, and stratigraphic relation of an in situ ashfall layer with an underlying desert pavement in Arena Valley, southern Victoria Land, indicate that a cold-desert climate has persisted in Arena Valley during the past 4.3 million years. These data indicate that the present East Antarctic Ice Sheet has endured for this time and that average temperatures during the Pliocene in Arena Valley were no greater than 3°C above present values. One implication is that the collapse of the East Antarctic Ice Sheet due to greenhouse warming is unlikely, even if global atmospheric temperatures rise to levels last experienced during mid-Pliocene times.

Two divergent hypotheses have been developed with regard to Pliocene paleoclimate and East Antarctic Ice Sheet dynamics. The first hypothesis, based on the ecology of warm-water marine diatoms and Nothofagus (Southern Beech) wood within Sirius Group glacial deposits in the Transantarctic Mountains, postulates that East Antarctic ice-sheet deglaciation occurred about 3.0 million years ago (Ma) (*1–8*). This hypothesis relies on two fundamental assumptions. The first is that reworked marine diatoms within the Sirius Group originated in ocean basins in the interior of East Antarctica and were subsequently transported into the forested Transantarctic Mountains by an expanded East Antarctic ice sheet. The second is that the biostratigraphy of sub-Antarctic deep-sea cores applies to far southern regions of interior Antarctica and hence can be used to apply confining ages to the Sirius Group. The latter assumption has apparently been confirmed by independent dating of volcanic ash in association with marine diatoms in the CIROS-2 core, southern Victoria Land (*1*). In sharp contrast, the second hypothesis postulates that the East Antarctic Ice Sheet has been relatively stable under persistent cold-desert conditions since around 14 Ma (*9*). This hypothesis is based on interpretation of the marine-oxygen isotope record, which shows little change at about 3.0 Ma. To evaluate these contradictory hypotheses, we examined Pliocene surficial sediments in Arena Valley, southern Victoria Land, for physical evidence of either warmer-than-present climates, including traces of meltwater (for example, rills, stream channels, mudflows, or levees), or persistent cold-desert conditions similar to the present climate (in which desert pavement, ultraxerous soil, and sand wedges are common).

D. R. Marchant, Institute for Quaternary Studies, University of Maine, Orono, ME 04469.
C. C. Swisher III, Institute of Human Origins, Geochronology Center, Berkeley, CA 94709.
D. R. Lux and D. P. West, Jr., Department of Geological Sciences, University of Maine, Orono, ME 04469.
G. H. Denton, Department of Geological Sciences and Institute for Quaternary Studies, University of Maine, Orono, ME 04469.

The Dry Valleys region of southern Victoria Land features about 4000 km^2 of predominantly ice-free, mountainous desert between the McMurdo Sound sector of the Ross Sea and the East Antarctic polar plateau (Fig. 1). Arena Valley, which lies at an average elevation of 1400 m in the Quartermain Mountains along the western margin of the Dry Valleys region, extends for 70 km^2 and is predominantly ice-free. A cold-based peripheral lobe of the upper Taylor Glacier extends 0.5 km into lower Arena Valley (*10*). Mean annual temperatures in Arena Valley are about −30°C, and precipitation is less than 45 mm of water equivalent (*11*). Under such climatic conditions ablation of Taylor Glacier at the valley mouth is entirely by sublimation (*10*). Glacial drifts, hummocky moraines,

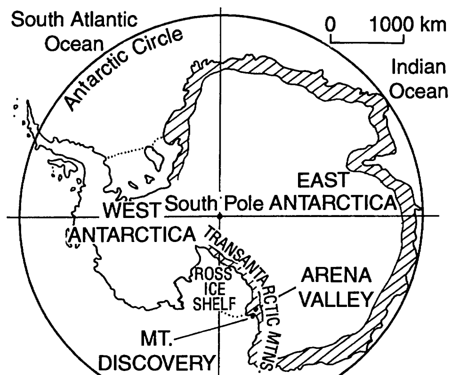

Fig. 1. Location map of Arena Valley, southern Victoria Land, Antarctica. Hatch marks represent the areal extent of surface-melting ablation zones in East Antarctica that we calculate would occur with a 22°C rise in atmospheric temperature over Antarctica. We suggest that Pliocene deglaciation of the East Antarctic Ice Sheet from elevated atmospheric temperatures would require a rise of the 0° isotherm to at least an elevation of 1600 m, or about 200 m elevation above the Arena Valley Ash deposit. Outside Antarctica, sediments that lie at or near the 0°C isotherm show a dynamic surficial stratigraphy.

talus cones, and colluvial deposits cover part of the floor and walls of Arena Valley. Conspicuously absent are geomorphic features indicative of liquid water, such as mudflows, levees, rills, lacustrine deposits, and stream channels, although they are common at elevations below about 800 m in the western Dry Valleys.

The Arena Valley Ash crops out on an extensive colluvial deposit with an average slope of 20°. The colluvium exhibits a well-developed ultraxerous soil profile and indurated salt pan, features suggestive of persistent desert conditions (*12*). The Arena Valley Ash deposit is about 25 cm thick and covers an area with a radius of about 10 m. It rests on a well-developed in situ desert pavement formed of an interlocking mosaic of gravel-sized ventifacts of Ferrar Dolerite, Beacon Supergroup sandstone, and orthoquartzite (Fig. 2). The ventifacts are commonly pitted and bear siliceous crusts and quartz rinds 5 to 10 mm thick; these features suggest that the pavement surface was subaerially exposed for a long time in a desert environment (*13*). A similar desert pavement now overlies the Arena Valley Ash and prevents erosion by wind deflation.

The Arena Valley Ash includes a lower basal unit and an upper ash-rich diamicton. The lower unit is structureless and consists of a thin layer (0.5 to 1.0 cm) of coarse-grained (0.5 to 1.0 mm) angular glass shards and volcanic crystals. The upper unit, approximately 20 to 25 cm thick, is composed of about 95% vesicular glass shards and volcanic crystals, 1 to 2% weathered quartz and dolerite sand-sized grains, and about 3% gravel-sized ventifacts of Beacon Supergroup sandstones and Ferrar Dolerite. Both units of the Arena Valley Ash contain less than 2.5% clay-sized grains. Glass shards are angular and unweathered, and volcanic crystals lack evidence of chemical etching (Fig. 3). X-ray microprobe analyses indicate that the glass shards (about 95% of the tephra by volume) are phonolitic. The crystals include anorthoclase, aegerine, subcalcic augite, and magnetite. Lavas on Mount Discovery, 110 km to the southeast of the Valley (Fig. 1), are largely phonolitic in composition (*14*), and this volcano is the most likely source for the Arena Valley Ash.

The composition of the lower unit and the preservation of the underlying in situ desert pavement indicate that the ash is a primary airfall deposit. The admixture of sand grains, ventifacts, and ash in the upper unit suggests that adjacent oversteepened colluvial deposits penecontemporaneously slumped on top of the airfall ash. The desert pavement overlying the Arena Valley Ash most probably formed by deflation of the upper ash-rich diamicton and concentration of enclosed ventifacts onto the ash surface.

The age of the Arena Valley Ash was determined both by $^{40}Ar/^{39}Ar$ dating of bulk anorthoclase separates (at the University of Maine) and by laser-fusion $^{40}Ar/^{39}Ar$ dating of single anorthoclase crystals (at the Geochronology Center). Analyses of bulk anorthoclase separates yielded a slightly U-shaped spectrum with a plateau age of 4.69 ± 0.10 Ma (Fig. 4). Similarly, 18 separate $^{40}Ar/^{39}Ar$ dates on single crystals of anorthoclase yielded an average age of 4.34 ± 0.025 Ma (SEM) (Table 1). We attribute the slightly older age of the bulk separate date to differences in calibration between the two laboratories, rare contamination from older detrital feldspar, or excess argon as suggested by the U-shaped $^{40}Ar/^{39}Ar$ spectrum (*15, 16*).

The age and stratigraphic relation of the Arena Valley Ash with the underlying ventifact pavement indicate that a desert climate existed in Arena Valley at 4.3 Ma. We suggest that a cold desert (as opposed to a hot desert) prevailed in Arena Valley at 4.3 Ma and has persisted to the present time for two reasons. First, landscape analysis indicates that surficial sediments that are coeval and older than the Arena Valley ash (which now are exposed over most of the Arena Valley) lack geomorphic evidence of liquid water. For example, there are no mudflow deposits, levees, rills, lacustrine deposits, or stream channels, although such features today are common elsewhere below an elevation of about 800 m in western Dry Valleys region. The mean annual air temperature at 800 m elevation is about −27°C [based on a recorded mean annual temperature of −19.8°C at about 100 m elevation at nearby Lake Vanda

Fig. 2. Photograph of the surficial volcanic ash deposit in west central Arena Valley. The vertical face has been cut back to expose the underlying buried desert pavement. A weathered, relict colluvial deposit (devoid of volcanic material) underlies the ash. This colluvial deposit overlies surficial sediments that crop out elsewhere over most of central Arena Valley. Hence, it represents one of the youngest surficial deposits in central and upper Arena Valley.

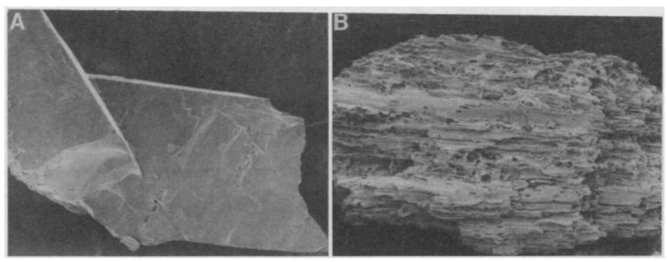

Fig. 3. Scanning electron microscope images of glass shards and anorthoclase crystals from the Arena Valley Ash. (**A**) shows an unweathered anorthoclase crystal (field of view is about 0.23 mm) (**B**) shows part of the vitric component of the ash (field of view is 0.30 mm). Glass shards removed from the upper unit of the Arena Valley ash show evidence of slight wind abrasion. Note the absence of etched crystals and authigenic minerals in the Pliocene-age, surficial Arena Valley Ash deposit.

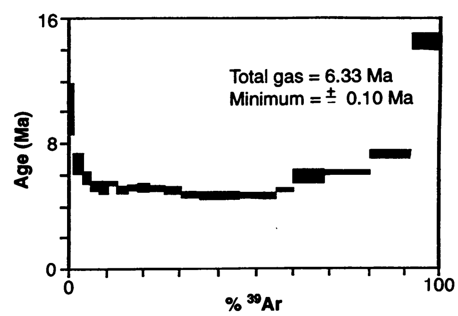

Fig. 4. Conventional $^{40}Ar/^{39}Ar$ release spectrum diagram from a bulk sample of anorthoclase separated from the Arena Valley Ash. The minimum age represents the mean of the five lowest age increments (which make up 25% of the total ^{39}Ar released). The total gas age is a weighted average of all the increments based on the amount of ^{39}Ar in each increment. The saddle-shaped release spectrum suggests that excess argon or xenocrystic contamination was present (*15, 16*). The incremental-heating experiment was carried out at the University of Maine on a Nuclide 6-60-SGA 1.25 mass spectrometer. The anorthoclase was irradiated at the Phoenix Reactor, University of Michigan, using FCT-3 biotite with an age of 27.68 as a monitor mineral. Anorthoclase crystals were removed from the Arena Valley Ash using standard magnetic density mineral separation techniques. Approximately 100 g of the ash yielded about 0.1 g of feldspar.

(*17*), and an average lapse rate of 1°C per 100 m elevation rise (*18*, *19*)]. In addition, there is no evidence of basal or surface melting of Taylor Glacier when it advanced several times into lower Arena Valley during at least the last 2.1 million years (*20*, *21*). The preservation of the Arena Valley Ash and underlying in situ ventifact pavement, together with the lack of geomorphic evidence for liquid water anywhere on the surface of unconsolidated sediments in Arena Valley, implies that cold-desert conditions persisted since the ash was deposited and indicates that mean annual temperatures in Arena Valley failed to rise above about −27°C. Second, the absence of clay-sized grains in the Arena Valley Ash is consistent with persistent cold-desert conditions since ash deposition. This is because the rate at which surficial ash deposits alter to clay minerals depends on atmospheric temperature and the abundance of pore water [rates are increased at high atmospheric temperatures and high pore-water pressures (*22*–*24*)]. For example, under humid temperate conditions in New Zealand, which are compatible with growth of Nothofagus, tephras older than about 50,000 years old are >60% clay (*22*–*24*).

Pliocene deglaciation would almost certainly have required the formation of extensive surface-melting ablation zones, analogous to the melting margins of terrestrial Northern Hemisphere ice sheets during the last termination (*25*). Formation of such ablation zones would demand a dramatic rise in the elevation of the 0°C isotherm, which now lies at an equivalent of 600 m below sea level for Arena Valley (*19*). A 2200 m rise in the elevation of the 0°C isotherm necessary to initiate a narrow band of surface melting up to 1600 m elevation near Arena Valley (Fig. 1) would require an atmospheric temperature rise of 11° to 31°C over Antarctica, for lapse rates of 0.5°C and 1.4°C per 100 m elevation rise, respectively (*26*). These estimates agree with those of ice-sheet models, which show that deglaciation of Antarctica requires an increase of mean annual surface temperatures by 17° to 19°C above present values (*18*, *27*). Our estimate for maximum potential Pliocene warmth in Arena Valley since 4.3 Ma is about 3°C above present values and is well below the minimum temperature rise necessary for either East Antarctic surface-melting ablation zones or ice-sheet collapse predicted by numerical models.

Postulated Nothofagus growth in the Transantarctic Mountains bears on the question of ice-sheet collapse. If verified, the growth of Nothofagus in the Transantarctic Mountains during Pliocene time would contribute strong evidence for East Antarctic deglaciation because today, north of the Antarctic Convergence, such trees occur in association with active glaciers possessing extensive surface-melting ablation zones. But Nothofagus, which today does not inhabit Antarctica, has strict ecological requirements. Nothofagus cannot survive mean annual temperatures below 5°C or minimum temperatures below −19°C for even a few hours (*28*). In view of the paleoclimatic inferences associated with the Arena Valley Ash, we argue that Nothofagus was eliminated from the Transantarctic Mountains before 4.3 Ma. Nothofagus cannot migrate long distances across salt water, and its seeds are not aerodynamic (*28*). As such, Nothofagus could not recolonize Antarctica after 4.3 Ma, even if atmospheric temperatures in the Transantarctic Mountains had warmed since 4.3 Ma. We conclude that postulated Nothofagus growth subsequent to 4.3 Ma in the Transantarctic Mountains is incorrect and cannot be used to support the warming necessary for surface-melting ablation zones required for ice-sheet collapse.

The geomorphological evidence argues strongly for continuous cold and dry climatic conditions in Arena Valley for at least the last 4.3 Ma. Such a view agrees with interpretations of the oceanic record (9) and points to the stability of the East Antarctic ice sheet under climatic warming of a few degrees. It is difficult at present to reconcile this conclusion with the hypothesis of Pliocene ice-sheet deglaciation (*1*–*8*). Perhaps it is possible that the Sirius Group antedates 3.0 Ma and that its enclosed diatoms have been emplaced by some mechanism other than glacier ice (*29*).

Table 1. Laser total fusion $^{40}Ar/^{39}Ar$ analyses of individual anorthoclase crystals from the Arena Valley Ash, carried out by the Institute of Human Origins Geochronology Center. Pristine euhedral crystals of anorthoclase were hand-picked from the Arena Valley Ash using a binocular microscope, treated with 7% hydrofluoric acid in an ultrasonic cleaner for 5 min to remove any altered clays or attached glass, followed by 10 min in distilled water, and then irradiated in the hydraulic rabbit core of the Omega West research reactor at Los Alamos National Laboratory for 4 hours. The calculated mean age of 4.343 ± 0.108 Ma (±1 standard deviation), ± 0.025 Ma (standard error of the mean) is based on 18 separate single-crystal analyses measured on a Mass Analyzer Product 215 noble-gas mass spectrometer, calibrated with monitor minerals Fish Canyon Sanidine and MMhb-I, with published ages of 27.84 Ma [modified from Cebula *et al.* (*30*)] and 520.4 Ma (*31*), respectively. Decay constants (λ) are those recommended by Steiger and Jager (*32*) and Dalrymple (*33*); Ca and K corrections used in this study as determined from laboratory salts are: $^{36}Ca/^{37}Ca = 2.557 \times 10^{-4} \pm 4.6 \times 10^{-6}$ $^{39}Ca/^{37}Ca = 6.608 \times 10^{-4} \pm 2.53 \times 10^{-5}$ and $^{40}K/^{39}K = 2.4 \times 10^{-3} \pm 7.0 \times 10^{-4}$

L no.	$^{37}Ar/^{39}Ar$†	$^{36}Ar/^{39}Ar$	$^{40}Ar^*/^{39}Ar$	%$^{40}Ar^*$	Age (Ma) ± 1σ
5075-01	0.03024	0.000228	0.81768	92.4	4.191 ± 0.203
5075-02	0.03814	0.000202	0.82572	93.3	4.232 ± 0.237
5075-03	0.04851	0.000014	0.86715	99.7	4.444 ± 0.250
5075-04	0.01887	0.000325	0.82006	89.4	4.203 ± 0.239
5075-05	0.02662	0.000519	0.82769	84.3	4.242 ± 0.278
5075-06	0.03051	0.000187	0.88239	94.1	4.522 ± 0.554
5075-07	0.02588	0.000054	0.86973	98.2	4.457 ± 0.422
5075-08	0.02000	0.000151	0.85239	94.9	4.368 ± 0.283
5075-09	0.03349	0.000274	0.82778	91.1	4.242 ± 0.418
5075-10	0.03700	0.000314	0.83205	90.0	4.264 ± 0.528
5075-11	0.03884	0.000126	0.86479	96.0	4.432 ± 0.271
5075-12	0.03493	0.000233	0.84062	92.5	4.308 ± 0.293
5075-13	0.04068	0.000183	0.85403	94.1	4.377 ± 0.334
5075-14	0.02144	0.000206	0.82717	93.1	4.239 ± 0.495
5075-15	0.04436	0.000025	0.88435	99.3	4.532 ± 0.366
5075-16	0.03135	0.000090	0.85779	97.0	4.396 ± 0.169
5075-17	0.03072	0.000082	0.85375	97.2	4.375 ± 0.359
5075-18	0.01180	0.000247	0.84824	91.9	4.347 ± 0.409
			Mean of 18 analyses =		4.343 ± 0.108

*Radiogenic. †$\lambda_\varepsilon + \lambda_\varepsilon' = 0.581 \times 10^{-10}\ yr^{-1}$; $\lambda_\beta = 4.962 \times 10^{-10}\ yr^{-1}$; and $^{40}K/^{40}K_{total} = 1.167 \times 10^{-4}$.

REFERENCES AND NOTES

1. P. J. Barrett, C. J. Adams, W. C. McIntosh, C. C. Swisher III, G. S. Wilson, *Nature* **359**, 816 (1992).
2. P. N. Webb and D. M. Harwood, *Quat. Sci. Rev.* **10**, 215 (1991).
3. ______, *Antarct. J. U.S.* **22**, 7 (1987).
4. P. N. Webb, *Antarct. Sci.* **1**, 3 (1990).
5. D. M. Harwood, *S. Afr. J. Sci.* **81**, 239 (1985).
6. ______, *Antarct. J. U.S.* **21**, 101 (1986).
7. P. N. Webb, D. M. Harwood, B. C. McKelvey, M. G. C. Mabin, J. H. Mercer, *ibid.*, p. 99.
8. P. N. Webb, D. M. Harwood, B. C. McKelvey, J. H. Mercer, L. D. Stott, *Geology* **12**, 287 (1984).
9. J. P. Kennett, *Marine Geology* (Prentice-Hall, Englewood Cliffs, NJ, 1982).
10. P. H. Robinson, *J. Glaciol.* **30**, 153 (1984).
11. J. G. Bockheim, *Geoderma* **28**, 239 (1982).
12. ______, *ibid.* **47**, 59 (1990).
13. R. Weed and S. A. Norton, in *Proceedings of the International Symposium on Environmental Biogeochemistry*, J. E. Bethelm, Ed. (Elsevier, Nancy, France, 1990), p. 327.
14. P. R. Kyle, *Am. Geophys. Union Antarct. Res. Ser.* **48**, 81 (1990).
15. I. McDougall and T. M. Harrison, *Geochronology and Thermochronology by the $^{40}Ar/^{39}Ar$ Method* (Oxford Univ. Press, New York, 1988).
16. Ph. G. Lo Bello *et al. Chem. Geol.* **66**, 61 (1987).

17. W. Schwerdtfeger, *Develop. Atmos. Sci.* **15**, (1984).
18. M. L. Prentice, J. L. Fastook, R. J. Oglesby, in *J. Geophys. Res.*, in press.
19. G. de Q. Robin, *Paleontol. Paleogeogr. Paleobiol.* **67**, 31 (1988).
20. D. R. Marchant, G. H. Denton, J. G. Bockheim, S. C. Wilson, A. R. Kerr, in preparation.
21. E. J. Brook, M. D. Kurz, R. P. Ackert, G. H. Denton, E. T. Brown, G. M. Raisbeck, F. Yiou, *Quat. Res.* **39**, 11 (1993).
22. D. J. Lowe, in *Rates of Chemical Weathering of Rocks and Minerals*, S. M. Colman and D. P. Dethier, Eds. (Academic Press, New York, 1986), pp. 265–330.
23. D. J. Lowe and C. S. Nelson, *Occas. Rep. 11.* (Department of Earth Sciences, University of Waikato, Hamilton, New Zealand, 1983).
24. K. S. Birrell and W. A. Pullar, *N. Z. J. Geol. Geophys.* **16**, 687 (1973).
25. G. H. Denton and T. J. Hughes, *The Last Great Ice Sheets* (Wiley-Interscience, New York, 1981).
26. J. P. F. Fortuin and J. Oerlemans, *Ann. Glaciol.* **14**, 78 (1990).
27. J. Oerlemans, *Nature* **297**, 550 (1982).
28. A. Sakai, *Ecol. Soc. S. America* **62**, 563 (1981).
29. D. E. Sugden, *Nature* **359**, 776 (1992).
30. G. T. Cebula *et al.*, *Terra Cognita* **6**, 139 (1986).
31. S. D. Samson and E. C. Alexander, *Chem. Geol. Isot. Geosci.* **66**, 27 (1987).
32. R. H. Steiger and E. Jager, *Earth Planet Sci. Lett.* **36**, 359 (1977).
33. G. B. Dalrymple, *Geology* **7**, 558 (1979).
34. This work was supported by the Division of Polar Programs, National Science Foundation.

29 September 1992; accepted 4 March 1993

Social Structure of Pilot Whales Revealed by Analytical DNA Profiling

Bill Amos,* Christian Schlötterer, Diethard Tautz

Long-finned pilot whales swim in large, extremely cohesive social groups known as pods. Molecular typing revealed that pod members form a single extended family. Mature males neither disperse from nor mate within their natal pods, a situation unusual for mammals. Such behavior could be explained in terms of inclusive fitness benefits gained by adult males helping the large number of female relatives with which they swim.

The inaccessibility of whales makes their social organization difficult to elucidate, yet such knowledge has important consequences for conservation and management. Cetacean mating systems have been inferred from comparisons with other mammals [see (*1*), for example]. However, given the unique marine ecology of whales, such extrapolations need to be substantiated by rigorous paternity testing.

A review of mammalian mating systems suggests that female reproductive behavior is highly constrained by the demands of gestation and lactation (*2*). Males can maximize their fitness in two ways: by mating with many females and by improving offspring number or quality through paternal care. In cases where females live in groups, competition between males tends to lead to polygyny (*2*). In virtually all cases, inbreeding is avoided by the dispersal of one or both sexes, usually the males (*3*). Our study shows that the pilot whale (*Globicephala melas*, Delphinidae) is unusual in its social organization: neither sex disperses from its natal group, and males show no evidence of reproductive dominance. Such a system raises interesting possibilities for the role of inclusive fitness in its evolution.

B. Amos, Department of Genetics, Cambridge University, Downing Street, Cambridge, United Kingdom CB2 3EH.
C. Schlötterer and D. Tautz, Zoologisches Institut der Universität München, Luisenstrasse 14, 8000 München 2, Germany.

*To whom correspondence should be addressed.

The long-finned pilot whale swims in large groups, or pods, often containing over 100 individuals. All age classes and both sexes are found in a pod, although there is a female sex bias among adults (*4*). Mating is broadly seasonal, with a diffuse peak in early summer (*4*). Pods are very cohesive, which can result in natural mass strandings and which allows them to be herded with boats. For centuries, this behavior has been exploited by coastal peoples to catch pilot whales for food. Today, only in the Faeroe Islands does this tradition continue, with a mean of some 1700 whales caught annually, mostly as entire pods (*5*). Molecular analysis of samples from this fishery suggests that pod members are related and that males seldom mate within the pods in which they are caught (*6*).

To clarify pilot whale structure and breeding behavior it is necessary to establish the following: (i) the degree of relatedness between pod members, (ii) whether adult males are related to the rest of the pod, and (iii) whether individual males mate with a few or with several females in any one pod. For this analysis we used a panel of highly variable microsatellite sequences (*7*).

Between 1986 and 1988, tissue samples were collected from many (presumed) complete pods from the Faeroese pilot whale drive fishery. Two pods were selected for detailed analysis on the basis of size and completeness of sampling (Miđvágur 240787, n = 103, and Leynar 220787, n = 90). Each sample was typed for one minisatellite locus [the *HMW* locus (*6*)] and six microsatellite loci. Of the microsatellite loci, five have between three and ten alleles per locus (Table 1). The sixth, however, is extremely polymorphic, with 54 alleles scored in the two study pods, 46% of which are unique to one or the other pod (Fig. 1).

The great variability of locus 468/469 allowed us to reassess male mating behavior. For 33 of 34 fetuses we could exclude all accompanying adult males as fathers, strengthening previous assertions that adult males rarely, if ever, mate within their home pods. Further, we compared paternal alleles among seven fetal cohorts (that is, fetuses conceived in the same pod in the same year; n = 6, 6, 12, 3, 10, 3, and 6 fetuses) sampled from four different pods. We found that 89% of paternal alleles were unique within a cohort, an observation incompatible with the idea that one or two males dominate mating (*8*). Given that a cohort's paternal alleles at the less variable minisatellite locus are nonrandom (*6*), our findings imply that groups of related males are the fathers.

To estimate the number of mother-offspring relationships in a pod, we designed a special analytical approach (*9*). The ob-

Table 1. Pilot whale microsatellite loci analyzed in this study. All primers flank a simple sequence stretch consisting either of GT or GA dinucleotide repeats.

Locus	Primer (5′ to 3′)	Number of alleles	Size range (base pairs)
199/200	TGAAATTCTTCATCAGT GTTAATGTAGGCAGACT	5	110 to 134
409/470	GTTTTGGTTGCTTGA TAAAAGACAGTGGCA	8	174 to 188
415/416	GTTCCTTTCCTTACA ATCAATGTTTGTCAA	6	222 to 234
417/418	GTGATATCATACAGTA ATCTGTTTGTCACATA	3	181 to 187
464/465	GGGGTTTCTCCTCTA TGATCTGCCAATAAGA	8	138 to 154
468/469	ACCCCAGAGAAAACA CAAGGTATTTCAGAA	54	87 to 185